Available online at www.sciencedirect.com
ScienceDirect
Journal of Power Sources 161 (2006) 1133–1153
JOURNAL OF POWER SOURCES
www.elsevier.com/locate/jpowsour

Performance/design formulation for a solid polymer based acid electrolyte hydrogen/air fuel cell

S.S. Sandhu [a,*], J.P. Fellner [b]

[a] *Department of Chemical and Materials Engineering, University of Dayton, 300 College Park, Dayton, OH 45469-0246, United States*
[b] *Air Force Research Laboratory, Propulsion Directorate, Plans and Analysis Branch, 1950 Fifth Street, Wright-Patterson AFB, OH 45433-7251, United States*

Received 21 April 2006; received in revised form 5 June 2006; accepted 6 June 2006
Available online 17 August 2006

Abstract

Mathematical development of preliminary performance/design equations for a hydrogen/air, solid polymer acid electrolyte based fuel cell is presented. The development is based on the principles of transport phenomena, intrinsic electrochemical kinetics, and classical thermodynamics. The developed formulation is intended to quantitatively describe the mass fraction profiles of the chemical species, hydrogen and oxygen, in the cell anode and cathode diffusion and electrocatalytic reaction layers as a function of the distance in the proton transport direction at an axial distance parallel to the cell anode or cathode channel flow. Given the cell geometry, chemical species and charge transport, and intrinsic electrochemical kinetic parameters, the developed formulation can be employed to compute the species local mass fluxes and predict the cell anode and cathode cell overvoltages for a desired geometric current density. The presented single cell performance predictive formulation has also been linked to the formulation needed to predict the performance of a stack of a number of identical PEMFCs connected in series.
© 2006 Elsevier B.V. All rights reserved.

Keywords: Fuel cells; Solid polymer; Performance model; Hydrogen; Air; Acid

1. Introduction

The current need, throughout our world, is power generation with greater energy efficiency and environmental protection. In general, fuel cells are a clean, efficient and quiet source of power generation. The polymer electrolyte membrane fuel cell, with hydrogen as the primary fuel, continues to be developed due to its low-temperature operation, rapid start-up and high power density. The polymer electrolyte membrane fuel cell (PEMFC; also called the proton exchange membrane fuel cell) converts the chemical energy of hydrogen and oxygen from air directly into electrical energy, with heat and water as by-products. In the near future, the PEMFCs, using hydrogen and air as reactants, are expected to replace the less efficient, pollutant (e.g., CO, NO_x, unburned hydrocarbons, soot) generating internal combustion engines burning fossil fuels acquired from dwindling terrestrial energy sources. Currently, the PEMFCs are not a commercially viable alternative to the internal combustion engines. However, an enhanced understanding of the various transport and electrochemical processes that occur within a PEM fuel cell, through mathematical modeling and experimental work, can help in the acceleration of commercialization of the PEMFC technology by providing gains in cost reduction, energy conversion efficiency, and power output.

Recent one-dimensional models of the PEMFC are given in Refs. [1–8]. These models provide useful insight and reasonable predictions of the cell performance in the low and intermediate current density ranges, but are not able to simulate the rapid electric potential drop observed experimentally at higher current densities. Two-dimensional models are given in Refs. [9–21]. Recent three-dimensional works are found in Refs. [22–33]. Most of these models found in the literature are shown to simulate the overall fuel cell performance (i.e., cell voltage versus current density) reasonably well. This agreement, irrespective of the dimensionality of a

* Corresponding author. Tel.: +1 937 229 2648.
E-mail address: Sarwan.Sandhu@notes.udayton.edu (S.S. Sandhu).

0378-7753/$ – see front matter © 2006 Elsevier B.V. All rights reserved.
doi:10.1016/j.jpowsour.2006.06.094

Nomenclature

a_α	activity of species α
a_{eff}	platinum surface area fraction effective for electrochemical reaction
a^{A}	active electrocatalyst surface area per unit ARL volume (m^{-1})
a^{C}	active electrocatalyst surface area per unit CRL volume (m^{-1})
A_i, B_i, C_i, D_i	heat capacity coefficients for an ideal gas i
c	total gas phase molar concentration (mol m^{-3})
c_α	gas phase molar concentration of species α (mol m^{-3})
D_α	gas phase mass diffusivity of species α ($\text{m}^2\,\text{s}^{-1}$)
E	cell voltage (V)
E_0	reaction activation energy (J mol^{-1})
f_1	defined by Eq. (39)
F	Faraday's constant (96,487 C g equiv.$^{-1}$)
F_1^{A}	defined by Eq. (31b)
F_1^{C}	defined by Eq. (82b)
ΔG	Gibbs free energy change (J mol^{-1})
ΔH	enthalpy of reaction (J mol^{-1})
ΔH_T	enthalpy of reaction given by Eq. (3) at temperature T (J mol^{-1})
$\Delta \dot{H}_{\text{t}}$	thermal energy production by Eq. (3) for combustion (W)
i_{geom}	geometric current density (A m^{-2})
$i_{0,\text{s}}$	intrinsic exchange current density (A m^{-2})
I_{t}	total current (A)
k_{c}	mass transfer coefficient (m s^{-1})
k_{e^-}	electronic conductivity ($\Omega^{-1}\,\text{m}^{-1}$)
k_0^{A}	frequency factor for hydrogen electrochemical reaction at the electrocatalyst surface ($\text{mol s}^{-1}\,\text{m}^{-2}\,\text{N m}^{-2}$)
L	length (m)
$m_{\text{Pt,geom}}$	platinum loading (kg m^{-2})
M_α	molecular weight of species α (kg mol^{-1})
n	number of cells in a series connected stack
$\dot{n}_\alpha$	mass flux of species α ($\text{kg m}^{-2}\,\text{s}^{-1}$)
$\dot{N}_\alpha$	molar flux of species α ($\text{mol m}^{-2}\,\text{s}^{-1}$)
$\dot{N}_{\text{in},\alpha}$	total molar flow rate in of species α (mol s^{-1})
$\dot{N}_{\text{exit},\alpha}$	total molar flow rate out of species α (mol s^{-1})
$\dot{N}_{\text{exit,t}}$	total molar flow rate out (mol s^{-1})
$-\Delta \dot{N}_{\text{H}_2}$	hydrogen consumption rate (mol s^{-1})
$\dot{Q}_{\text{remove}}$	thermal energy needed to be removed to remain isothermal (W)
r_{Pt}	platinum average spherical particle radius (m)
r_α	electrochemical molar reaction rate of species α per unit of catalyst surface ($\text{mol s}^{-1}\,\text{m}^{-2}$)
R_α	electrochemical molar reaction rate of species α per unit geometric volume ($\text{mol s}^{-1}\,\text{m}^{-3}$)
$R_{\alpha,\text{mass}}$	electrochemical mass reaction rate of species α per unit geometric volume ($\text{kg s}^{-1}\,\text{m}^{-3}$)
s	platinum specific surface area ($\text{m}^2\,\text{kg}^{-1}$)
p_α	partial pressure of species α (N m^{-2})
P	gas mixture total pressure (N m^{-2})
PEMFC	polymer electrolyte membrane fuel cell or proton exchange membrane fuel cell
R	universal gas constant ($8.314\,\text{J mol}^{-1}\,\text{K}^{-1}$ or $8.314\,\text{N m}^{-2}\,\text{m}^3\,\text{mol}^{-1}\,\text{K}^{-1}$)
T	Temperature (K)
W	width (m)
$\dot{W}_{\text{electric}}$	electric power (W)
x	coordinate axis for cell length or distance along x axis (m)
y	coordinate axis for cell width or distance along y axis (m)
y_α	mole fraction of species α
z	coordinate axis for cell thickness or distance along z axis (m)
$z^{\text{A}}_{\text{near-side}}$	$\delta^{\text{ACH}} + \delta^{\text{ADL}}$ (m)
$z^{\text{A}}_{\text{far-side}}$	$\delta^{\text{ACH}} + \delta^{\text{ADL}} + \delta^{\text{A}}$ (m)

z_{ns}^{CRL} $\delta^{ACH} + \delta^{ADL} + \delta^{A} + \delta^{SEP}$ (m)
z_{fs}^{CRL} $\delta^{ACH} + \delta^{ADL} + \delta^{A} + \delta^{SEP} + \delta^{C}$ (m)
z_{ns}^{CDL} $\delta^{ACH} + \delta^{ADL} + \delta^{A} + \delta^{SEP} + \delta^{C}$ (m)
z_{fs}^{CDL} $\delta^{ACH} + \delta^{ADL} + \delta^{A} + \delta^{SEP} + \delta^{C} + \delta^{CDL}$(m)

Greek letters

α defined by Eq. (35c)
α_1 defined by Eq. (84b)
α_a anodic charge transfer coefficient
α_c cathodic charge transfer coefficient
δ thickness (m)
ε volume fraction or void fraction
ζ defined by Eq. (35b)
ζ_{H_2O} moles of water transported to CRL per mole of H^+ migrating from ARL to CRL
η voltage loss (V)
$\eta_{thermal}$ thermal efficiency
ν_i stoichiometric coefficient
ρ gas phase density (kg m^{-3})
σ ionic conductivity (ohm^{-1} m^{-1})
$\tau_{p(g)}$ tortuosity factor of gas-filled pores
φ electric potential in ARL (V)
$\Delta\varphi$ Galvanic electric potential difference in ARL (V)
ϕ electric potential in CRL (V)
$\Delta\phi$ Galvanic electric potential difference in CRL (V)
ω_α mass fraction of species α

Superscripts

A anode reaction layer
ACH anode channel
ACH–DL anode channel + anode diffusion layer
ACH–DL–RL anode channel + anode diffusion layer + anode reaction layer
ADL anode diffusion layer
ARL anode reaction layer
cell cell
contact contact resistance
C cathode reaction layer
CCH cathode channel
CDL cathode diffusion layer
CRL cathode reaction layer
m reaction order
sat'd vapor saturated vapor
stack number of n cells in series
SEP solid polymer electrolyte membrane
t total
° standard state

Subscripts

ave average
carbon carbon material used in electrodes
e^- electronic
eff effective
electrolyte solid polymer electrolyte
fs far side
g gas
geom geometric

H^+	protonic or ionic
ns	near side
rev	reversible
$p_{H_2,0}$	reference partial pressure of hydrogen
Pt	bulk platinum catalyst
t	total
z	coordinate axis for cell thickness
T	cell temperature
T_0	reference temperature (298.15 K)
0	reference condition
α	H_2, N_2, CO_2, H_2O, etc.
α-δ^{ACH}	chemical species α at the ACH/ADL interface
β	H_2, N_2, CO_2, H_2O, etc.
Ω	ohmic

model, is quite likely due to the adjustment of one or more parameter values. A three-dimensional modeling work [34] has been validated against local current density data obtained experimentally with a segmented cell. All these models attempt to model a PEMFC in a realistic fashion without resulting in too much of computational expense.

A mathematical formulation is developed below for a hydrogen/air PEMFC utilizing, for example, Nafion, PBO(poly(*p*-phenylene-2,6-benzobisoxazole))/PBI (poly(benzimidazole)) based phosphoric acid, or sulfonated polyarylene ether or Nafion–Teflon–$Zr(HPO_4)_2$ as an electrolyte. This two-dimensional model, originally developed for a PEMFC fueled by hydrogen gas, can be extended to predict the performance of PEMFC fueled by a gas mixture containing hydrogen, carbon monoxide, small amount of oxygen, carbon dioxide and nitrogen as found in the gas mixture issuing from a reformer dedicated for the production of fuels for fuel cell applications [35]. Isothermal, steady-state conditions have been assumed.

2. Mathematical formulation

Fig. 1 shows the schematic of a single proton exchange membrane fuel cell (PEMFC). Operation of such a PEMFC is assumed to be under the isothermal and steady-state conditions. Hydrogen gas or gas mixture, containing hydrogen, nitrogen, carbon dioxide, etc., from a reformer enters the anode channel and flows in the *x*-direction. At any *x*-location, hydrogen diffuses from the anode channel bulk flow to the porous carbon anode diffusion layer (ADL). Then, it diffuses through the ADL to the interface between the

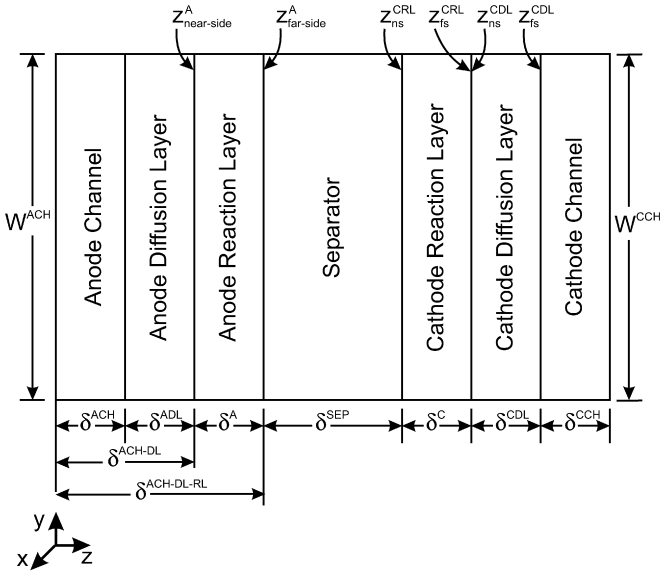

Fig. 1. Schematic of a single fuel cell. *Note*: The *x*-direction is ⊥ the *y*–*z* plane. Fuel and oxidant gas streams in the anode and cathode channel are parallel to the *x*-direction. L^{ACH}, L^{CCH}: anode and cathode channel length, respectively, parallel to the *x*-axis. δ^{ACH}, δ^{ADL}, δ^{A}, δ^{SEP}, δ^{C}, δ^{CDL}, and δ^{CCH} are the dimensions of anode channel, anode diffusion layer, anode reaction layer, solid polymer electrolyte membrane, cathode reaction layer, cathode diffusion layer, and cathode channel, respectively, parallel to the *z*-axis. W^{ACH} and W^{CCH} are the anode and cathode channel dimensions, respectively, parallel to the *y*-axis.

ADL and the anode reaction layer (ARL). The porous reaction layer is assumed to be composed of the catalytic platinum particles, in contact with an acid solid polymer electrolyte such as Nafion or PBO/PBI electrolyte, dispersed on the porous carbon granules. Hydrogen diffuses toward the interface between the ARL and solid polymer electrolyte separator layer sandwiched between the anode and cathode reaction layers. In the ARL, hydrogen, while it diffuses, is consumed via the overall electrochemical reaction given by Eq. (1). The generated electrons enter an external electric circuit to pass through an external electrical load. The generated protons, H^+, migrate internally through the electrolyte separator to the porous cathode reaction layer (CRL) where they cause reduction of oxygen in the presence of electrons that return from the external electric load to the cathode reaction layer.

Atmospheric air, containing varying degrees of water vapor, enters the cathode-side flow channel. At any x-location in the flow channel, oxygen diffuses toward the cathode reaction layer in a negative z-direction. Oxygen first diffuses through the chemical species concentration boundary layer to the porous carbon cathode diffusion layer (CDL). The chemical species concentration boundary layer may or may not prevail at the porous surface of the CDL depending on the oxygen reduction rate in the CRL and the cathode channel flow Reynolds number value. It then diffuses through the CDL to the interface between the CDL and relatively thinner CRL. The porous CRL is assumed to be composed of the catalytic platinum particles, in contact with an acid solid polymer electrolyte, for example, Nafion or PBO/PBI, dispersed on the porous carbon granules. In the CRL, oxygen diffuses toward the interface between the CRL and solid polymer acid electrolyte separator layer, while it is simultaneously consumed via the following overall electrochemical reduction reaction given by Eq. (2). The electrochemically produced water in the cathode reaction layer diffuses through the cathode reaction and diffusion layers. It, then, diffuses through the species concentration boundary layer prevailing at the porous CDL surface to join the cathode channel bulk flow. It is here noted that the oxygen mass transport is in the direction of decreasing z while water vapor transport is in the opposite direction. Transport of the gaseous species through the solid polymer electrolyte separator layer is assumed to be negligibly small.

Given below are the main mathematical model equations. One may find the detail behind the formulation development elsewhere [36].

The half cell reactions at the anode and cathode electrocatalytic reaction layers, respectively, are:

$$H_2 \rightleftarrows 2H^+ + 2e^- \tag{1}$$

$$\tfrac{1}{2}O_{2(g)} + 2H^+ + 2e^- \rightleftarrows H_2O_{(g)} \tag{2}$$

The overall cell reaction is

$$H_{2(g)} + \tfrac{1}{2}O_{2(g)} \rightleftarrows H_2O \tag{3}$$

The reversible cell voltage is given by

$$E_{\text{rev}}^{\text{cell}} = E^\circ + \frac{RT}{2F}\ln\left[\frac{(p_{H_2}/p^\circ)(p_{O_2}/p^\circ)^{1/2}}{a_{H_2O}}\right] \tag{4}$$

In the denominator of Eq. (4), the constant two corresponds to 2 mol of H^+ or e^- per 1 mol of H_2 consumed electrochemically. The standard-state reversible cell voltage, E°, at the cell temperature, T, is given by

$$E^\circ = \frac{-\Delta G_T^\circ}{2F} \tag{5}$$

For convenience, ΔG_T°, can be computed, with negligibly small error, from the following equation since it can be assumed that $(\partial \Delta G_T^\circ/\partial T)_P$ is approximately constant over the range of interest [37]:

$$\Delta G_T^\circ = \left(\frac{T}{T_0}\right)(\Delta G_{T_0}^\circ - \Delta H_{T_0}^\circ) + \Delta H_{T_0}^\circ \tag{6}$$

Total ohmic voltage drop in the electrolyte separator and anode and cathode diffusion and electrocatalytic reaction layers is given by

$$\eta_\Omega^{\text{t}} = \eta_\Omega^{\text{SEP}} + (\eta_\Omega^{\text{ADL}} + \eta_\Omega^{\text{CDL}}) + (\eta_\Omega^{\text{A}} + \eta_\Omega^{\text{C}}) + \eta^{\text{contact}} \tag{7}$$

The ohmic voltage loss due to the resistance to H^+ transport in the electrolyte separator (SEP) layer, η_Ω^{SEP} is computed from:

$$\eta_\Omega^{\text{SEP}} = i_{\text{geom}}\frac{\delta^{\text{SEP}}}{\sigma_{H^+,\text{eff,electrolyte}}} \tag{8}$$

The ohmic voltage drop in the anode and cathode diffusion layers are given by

$$\eta_\Omega^{\text{ADL}} = i_{\text{geom}}\frac{\delta^{\text{ADL}}}{k_{e^-,\text{eff}}^{\text{ADL}}} \tag{9a}$$

where

$$k_{e^-,\mathrm{eff}}^{\mathrm{ADL}} = \varepsilon_{\mathrm{carbon}}^{\mathrm{ADL}} k_{e^-,\mathrm{eff,carbon}}^{\mathrm{ADL}} \tag{9b}$$

and

$$\eta_{\Omega}^{\mathrm{CDL}} = i_{\mathrm{geom}} \frac{\delta^{\mathrm{CDL}}}{k_{e^-,\mathrm{eff}}^{\mathrm{CDL}}} \tag{10a}$$

where

$$k_{e^-,\mathrm{eff}}^{\mathrm{CDL}} = \varepsilon_{\mathrm{carbon}}^{\mathrm{CDL}} k_{e^-,\mathrm{eff,carbon}}^{\mathrm{CDL}} \tag{10b}$$

The ohmic drop in the anode reaction layer due to the resistance to H^+ and electron conduction is given by

$$\eta_{\Omega}^{\mathrm{A}} = \eta_{H^+,\Omega}^{\mathrm{A}} + \eta_{e^-,\Omega}^{\mathrm{A}} \tag{11a}$$

$$= \frac{i_{\mathrm{geom}}\delta^{\mathrm{A}}}{2}\left(\frac{1}{\sigma_{H^+,\mathrm{eff}}^{\mathrm{A}}} + \frac{1}{k_{e^-,\mathrm{eff}}^{\mathrm{A}}}\right) \tag{11b}$$

where

$$\sigma_{H^+,\mathrm{eff}}^{\mathrm{A}} = \varepsilon_{\mathrm{electrolyte}}^{\mathrm{A}} \sigma_{H^+,\mathrm{eff,electrolyte}}^{\mathrm{A}} \tag{11c}$$

and

$$k_{e^-,\mathrm{eff}}^{\mathrm{A}} = \varepsilon_{\mathrm{carbon}}^{\mathrm{A}} k_{e^-,\mathrm{eff,carbon}}^{\mathrm{A}} \tag{11d}$$

The factor 2 in the denominator of the right-hand side expression of the equal sign in Eq. (11b) appears to account for the fact that the H^+ flux is zero at $z = z_{\text{near-side}}^{\mathrm{A}}$ just on the 'minus side' of the interface between the anode diffusion and reaction layers and it corresponds to i_{geom} at $z = z_{\text{far-side}}^{\mathrm{A}}$, just on the 'plus side' of the interface between the anode reaction and polymer electrolyte separator layers. The electron flux is zero at $z = (z_{\text{far-side}}^{\mathrm{A}})^{+}$ and it corresponds to i_{geom} at $z = (z_{\text{near-side}}^{\mathrm{A}})^{-}$. This means that the arithmetic average current density, $i_{\mathrm{geom}}/2$, has been used in Eq. (11b) to estimate $\eta_{\Omega}^{\mathrm{A}}$.

The ohmic voltage drop in the cathode reaction layer due to the resistance to H^+ and electron conduction is given by

$$\eta_{\Omega}^{\mathrm{C}} = \eta_{H^+,\Omega}^{\mathrm{C}} + \eta_{e^-,\Omega}^{\mathrm{C}} \tag{12a}$$

$$= \frac{i_{\mathrm{geom}}\delta^{\mathrm{C}}}{2}\left(\frac{1}{\sigma_{H^+,\mathrm{eff}}^{\mathrm{C}}} + \frac{1}{k_{e^-,\mathrm{eff}}^{\mathrm{C}}}\right) \tag{12b}$$

where

$$\sigma_{H^+,\mathrm{eff}}^{\mathrm{C}} = \varepsilon_{\mathrm{electrolyte}}^{\mathrm{C}} \sigma_{H^+,\mathrm{eff,electrolyte}}^{\mathrm{C}} \tag{12c}$$

and

$$k_{e^-,\mathrm{eff}}^{\mathrm{C}} = \varepsilon_{\mathrm{carbon}}^{\mathrm{C}} k_{e^-,\mathrm{eff,carbon}}^{\mathrm{C}} \tag{12d}$$

Voltage losses associated with the contact resistances between the various cell layers is given by η^{contact} and is due to the lack of 'perfect contact' and is a function of stack pressure. Perfect contact, as a first order, is assumed in this analysis.

2.1. The fuel cell anode-side formulation

The flux of a chemical species α in the z-direction at an x-location through the fluid phase concentration boundary layer prevailing at the porous anode carbon diffusion layer (ADL), in general, is given by

$$\dot{N}_{\alpha,\mathrm{eff},z} = k_{\mathrm{c},\alpha}^{\mathrm{ACH}} \varepsilon_{\mathrm{g}}^{\mathrm{ADL}} (c_{\alpha}^{\mathrm{ACH}} - c_{\alpha-\delta^{\mathrm{ACH}}}) \tag{13a}$$

where $\alpha = H_2, N_2, CO_2, H_2O$, etc. The mass flux of a chemical species α in the z-direction through the concentration boundary layer is given by

$$\dot{n}_{\alpha,\mathrm{eff},z} = \dot{N}_{\alpha,\mathrm{eff},z} M_{\alpha} = k_{\mathrm{c},\alpha}^{\mathrm{ACH}} \varepsilon_{\mathrm{g}}^{\mathrm{ADL}} M^{\mathrm{ACH}} c^{\mathrm{ACH}} (\omega_{\alpha}^{\mathrm{ACH}} - \omega_{\alpha-\delta^{\mathrm{ACH}}}) \tag{13b}$$

$$M^{\mathrm{ACH}} = \sum_{\alpha} y_{\alpha}^{\mathrm{ACH}} M_{\alpha} \tag{13c}$$

$$y_{\alpha}^{\mathrm{ACH}} = \frac{\dot{N}_{\alpha}^{\mathrm{ACH}}}{\sum_{\alpha} \dot{N}_{\alpha}^{\mathrm{ACH}}} \tag{13d}$$

$$\omega_{\alpha}^{\mathrm{ACH}} = \frac{y_{\alpha}^{\mathrm{ACH}} M_{\alpha}}{M^{\mathrm{ACH}}} \tag{13e}$$

$$c^{\mathrm{ACH}} = \frac{P^{\mathrm{ACH}}}{RT} \tag{13f}$$

The value of the mass transfer coefficient, $k_{\mathrm{c},\alpha}^{\mathrm{ACH}}$, can be determined using standard semiempirical equations [36,38].

The gas mixture density in the anode channel can be computed from:

$$\rho = \frac{P^{\mathrm{ACH}}}{RT} \sum_{\alpha} y_{\alpha}^{\mathrm{ACH}} M_{\alpha} \tag{14}$$

The mass flux equation for transport of a chemical species through the porous carbon anode diffusion layer is given as

$$\dot{n}_{\alpha,\mathrm{eff},z} = -\rho D_{\alpha,\mathrm{eff}}^{\mathrm{ADL}} \frac{\mathrm{d}\omega_{\alpha}}{\mathrm{d}z} + \omega_{\alpha} \sum_{\beta} \dot{n}_{\beta,\mathrm{eff},z} \tag{15a}$$

where α, $\beta = H_2$, N_2, CO_2, H_2O, etc., and

$$D_{\alpha,\mathrm{eff}}^{\mathrm{ADL}} = \frac{D_{\alpha-\mathrm{gas}}^{\mathrm{ADL}} \varepsilon_{\mathrm{g}}^{\mathrm{ADL}}}{\tau_{\mathrm{p(g)}}^{\mathrm{ADL}}} \tag{15b}$$

Correction for the Knudsen diffusion effect on the species transport in the pores should be included if the average pore radius is less than 10 nm or 100 Å.

For the assumption of $\dot{n}_{\beta,\mathrm{eff},z} = 0$ (when $\beta = N_2$, CO_2, H_2O), with $\alpha = H_2$, Eq. (15a) reduces to

$$\dot{n}_{\mathrm{H_2},\mathrm{eff},z} = \frac{\rho D_{\mathrm{H_2},\mathrm{eff}}^{\mathrm{ADL}}}{(1-\omega_{\mathrm{H_2}})} \left(\frac{-\mathrm{d}\omega_{\alpha}}{\mathrm{d}z} \right) \tag{16}$$

Eq. (16) is solved for ω_{H_2}, with the boundary condition, at $z = \delta^{\mathrm{ACH}}$, $\omega_{\mathrm{H_2}} = \omega_{\mathrm{H_2},\delta^{\mathrm{ACH}}}$ = mass fraction of hydrogen in the gas mixture at the porous surface of the carbon ADL facing the anode channel flow. The result is

$$\omega_{\mathrm{H_2}} = 1 - (1 - \omega_{\mathrm{H_2},\delta^{\mathrm{ACH}}}) \exp \left[\left(\frac{\dot{n}_{\mathrm{H_2},\mathrm{eff},z}}{\rho D_{\mathrm{H_2},\mathrm{eff}}^{\mathrm{ADL}}} \right) (z - \delta^{\mathrm{ACH}}) \right] \tag{17}$$

valid for $\delta^{\mathrm{ACH}} \le z \le (\delta^{\mathrm{ACH}} + \delta^{\mathrm{ADL}})$. Eq. (13b) is used to eliminate $\omega_{\mathrm{H_2},\delta^{\mathrm{ACH}}}$ from Eq. (17) to obtain:

$$\omega_{\mathrm{H_2}} = 1 - \left\{ 1 - \omega_{\mathrm{H_2}}^{\mathrm{ACH}} + \frac{\dot{n}_{\mathrm{H_2},\mathrm{eff},z}}{k_{\mathrm{c,H_2}}^{\mathrm{ACH}} \varepsilon_{\mathrm{g}}^{\mathrm{ADL}} M^{\mathrm{ACH}} c^{\mathrm{ACH}}} \right\} \exp \left[\left(\frac{n_{\mathrm{H_2},\mathrm{eff},z}}{\rho D_{\mathrm{H_2},\mathrm{eff}}^{\mathrm{ADL}}} \right) (z - \delta^{\mathrm{ACH}}) \right] \tag{18a}$$

valid for $\delta^{\mathrm{ACH}} \le z \le (\delta^{\mathrm{ACH}} + \delta^{\mathrm{ADL}})$. Eq. (18a) can be employed to calculate the mass fraction of hydrogen, ω_{H_2}, as a function of distance z in the porous carbon anode diffusion layer provided $\dot{n}_{\mathrm{H_2},\mathrm{eff},z}$, corresponding to a current density, i_{geom}, and the anode channel bulk gas concentration of H_2, $\omega_{\mathrm{H_2}}^{\mathrm{ACH}}$, at an x-location are known.

For the situation of non-zero mass flux of water vapor in the anode diffusion layer, the following derived expression should be used to compute the hydrogen mass fraction profile in the anode diffusion layer [40]:

$$\omega_{\mathrm{H_2}} = \Theta - \left\{ \Theta - \omega_{\mathrm{H_2}}^{\mathrm{ACH}} + \frac{\dot{n}_{\mathrm{H_2},\mathrm{eff},z}}{k_{\mathrm{c,H_2}}^{\mathrm{ACH}} \varepsilon_{\mathrm{g}}^{\mathrm{ADL}} M^{\mathrm{ACH}} c^{\mathrm{ACH}}} \right\} \exp \left[\left(\frac{\dot{n}_{\mathrm{H_2},\mathrm{eff},z}}{\rho D_{\mathrm{H_2},\mathrm{eff}}^{\mathrm{ADL}}} \right) \Theta (z - \delta^{\mathrm{ACH}}) \right] \tag{18b}$$

where $\Theta = 1/(1 + 18\zeta_{\mathrm{H_2O}})$.

In the anode reaction layer (ARL), hydrogen is transported as well as consumed via the electrochemical reaction at the active catalyst platinum-electrolyte interface to produce H^+ ions and electrons. The hydrogen consumption rate:

$$(-r_{\mathrm{H_2}}^{\mathrm{A}}) = \left(\frac{i_{0,\mathrm{s}}^{\mathrm{A}}}{2F} \right) \exp \left(\frac{\alpha_{\mathrm{a}}^{\mathrm{A}} |\eta^{\mathrm{A}}| F}{RT} \right) \tag{19}$$

where the anodic intrinsic exchange current density is given by

$$i_{0,s}^{A} = i_{0,s,T_0,p_{H_2,0}}^{A} \exp\left[\frac{E_0^A}{R}\left(\frac{1}{T_0}-\frac{1}{T}\right)\right]\left(\frac{p_{H_2}}{p_{H_2,0}}\right)^m \tag{20}$$

and

$$|\eta^A| = |E^A - E_{rev}^A| = |\Delta\varphi^A - \Delta\varphi_{rev}^A| = |(\varphi_{Pt}-\varphi_{electrolyte})^A - (\varphi_{Pt}-\varphi_{electrolyte})_{rev}^A| \tag{21}$$

Note that when an impurity, for example CO, is present in the hydrogen fuel feed mixture above 10 ppm [39], it acts as the poison for the hydrogen oxidation or de-electronation reaction on the cell anode surface. Its effect to decrease the rate of hydrogen de-electronation on the anode surface should be accounted for using an experimentally determined kinetic deactivation function in Eq. (19). For the consumption of hydrogen by the first-order reaction, $m = 1$ in Eq. (20).

If it is assumed that the catalyst crystallites are spherical and their average size is r_{Pt}^A (radius), the platinum surface area per unit mass of platinum crystallites is given by

$$s^A = \frac{4\pi(r_{Pt}^A)^2}{(4/3)\pi(r_{Pt}^A)^3\rho_{Pt}} = \frac{3}{r_{Pt}^A\rho_{Pt}} \tag{22}$$

If some fraction of the catalyst surface is not in contact with the electroactive regions of the polymer electrolyte; then, the reaction effective electrocatalyst interfacial area is given by

$$s_{eff}^A = a_{eff}^A s^A \tag{23}$$

For a platinum loading in the anode reaction layer of m_{Pt}^A, the electrochemical reaction active electrocatalyst surface area per unit anode reaction layer volume is given by

$$a^A = s_{eff}^A m_{Pt}^A \tag{24}$$

The relation of m_{Pt}^A to the catalyst loading per unit geometric area, $m_{Pt,geom}^A$, of the anode reaction layer of thickness, δ^A, is given by

$$m_{Pt,geom}^A = \delta^A m_{Pt}^A \tag{25}$$

The molar hydrogen consumption rate per unit anode reaction layer volume, $-R_{H_2}^A$, is given by

$$-R_{H_2}^A = \left(\frac{i_{0,s}^A}{2F}\right) a^A \exp\left[\frac{\alpha_a^A|\eta^A|F}{RT}\right] \tag{26a}$$

The hydrogen consumption rate in mass units is given by

$$-R_{H_2,mass}^A = (-R_{H_2}^A)M_{H_2} = \left(\frac{i_{0,s}^A}{2F}\right) a^A M_{H_2} \exp\left[\frac{\alpha_a^A|\eta^A|F}{RT}\right] \tag{26b}$$

For the assumption of hydrogen transport in the relatively thin anode reaction layer via molecular mass diffusion, the hydrogen mass transport flux in the z-direction in the anode reaction layer is given by

$$\dot{n}_{H_2,eff,z}^{ARL} = \rho D_{H_2,eff}^{ARL}\left(\frac{-d\omega_{H_2}}{dz}\right) \tag{27}$$

A mass balance for hydrogen over a thin spatial element in the anode reaction layer was applied to obtain the following differential equation accounting for the simultaneous transport and consumption of hydrogen via electrochemical reaction:

$$\frac{d\dot{n}_{H_2,eff,z}^{ARL}}{dz} = -\left(\frac{i_{0,s}^A}{2F}\right) a^A M_{H_2} \exp\left[\frac{\alpha_a^A|\eta^A|F}{RT}\right] \tag{28}$$

On substitution for $\dot{n}_{H_2,eff,z}^{ARL}$ from Eq. (27) into Eq. (28), for the assumption of constant ($\rho D_{H_2,eff}^{ARL}$) [40], the following differential equation was obtained:

$$\frac{d^2\omega_{H_2}}{dz^2} = \left(\frac{i_{0,s}^A}{2F}\right)\left(\frac{a^A M_{H_2}}{\rho D_{H_2,eff}^{ARL}}\right) \exp\left(\frac{\alpha_a^A|\eta^A|F}{RT}\right) \tag{29}$$

Using:

$$\frac{i_{0,s}^{A}}{2F} = k_0^{A} \exp\left(\frac{-E_0^{A}}{RT}\right) p_{H_2} \tag{30a}$$

$$= k_0^{A} \exp\left(\frac{-E_0^{A}}{RT}\right) \left(\frac{M^{ACH} P^{ACH}}{M_{H_2}}\right) \omega_{H_2} \tag{30b}$$

Eq. (29) was transformed to the following form:

$$\frac{d^2\omega_{H_2}}{dz^2} = F_1^{A} \omega_{H_2} \tag{31a}$$

where

$$F_1^{A} = \left[\frac{M^{ACH} P^{ACH} a^{A}}{\rho D_{H_2,eff}^{ARL}}\right] \left[k_0^{A} \exp\left(-\left(\frac{E_0^{A} - \alpha_a^{A}|\eta^{A}|F}{RT}\right)\right)\right] \tag{31b}$$

where k_0^{A} = frequency factor for the hydrogen de-electronation or oxidation reaction at the electrocatalyst surface for the assumed first-order reaction. Eq. (31a) was solved using the boundary conditions: at $z = \delta^{ACH} + \delta^{ADL}$, $\omega_{H_2} = \omega_{H_2,\delta^{ACH-ADL}}^{+}$, the hydrogen mass fraction on positive side of the interface between the anode diffusion and reaction layers; at $z = \delta^{ACH} + \delta^{ADL} + \delta^{ARL}$, $(d\omega_{H_2}/dz)^{-} = 0$. The resulting solution to compute ω_{H_2} as a function of the distance z is given as

$$\omega_{H_2} = \omega_{H_2,\delta^{ACH-DL}}^{+} \left[\frac{\cosh\left(\sqrt{F_1^{A}} z\right)}{\cosh\left(\sqrt{F_1^{A}} \delta^{ACH-DL}\right)}\right] \left[\frac{1 - \tanh\left(\sqrt{F_1^{A}} z\right) \tanh\left(\sqrt{F_1^{A}} \delta^{ACH-DL-RL}\right)}{1 - \tanh\left(\sqrt{F_1^{A}} \delta^{ACH-DL}\right) \tanh\left(\sqrt{F_1^{A}} \delta^{ACH-DL-RL}\right)}\right] \tag{32}$$

or, further simplification yields:

$$\omega_{H_2} = \omega_{H_2,\delta^{ACH-DL}}^{+} \left[\frac{\cosh\left(\sqrt{F_1^{A}} (\delta^{ACH-DL-RL} - z)\right)}{\cosh\left(\sqrt{F_1^{A}} (\delta^{ACH-DL-RL} - \delta^{ACH-DL})\right)}\right]$$

Eq. (32) is valid for $\delta^{ACH-DL} < z \le \delta^{ACH-DL-RL}$. The solution given in Eq. (32) was obtained using the assumption that variation in $|\eta^{A}|$ with respect to z in a thin reaction layer is negligibly small. In general, activity of hydrogen on the negative and positive sides of the interface between the anode diffusion and reaction layers can be assumed to be the same if hydrogen gas is present in different phases. If it is assumed that hydrogen is present in the gas phase across the interface between the anode diffusion and reaction layers; then, it is reasonable to assume:

$$\omega_{H_2,\delta^{ACH-DL}}^{-} = \omega_{H_2,\delta^{ACH-DL}}^{+} \tag{33}$$

Using Eq. (18a), the following equation was obtained:

$$\omega_{H_2,\delta^{ACH-DL}}^{+} = \omega_{H_2,\delta^{ACH-DL}}^{-} = 1 - \left\{1 - \omega_{H_2}^{ACH} + \frac{\dot{n}_{H_2,eff,z}}{k_{c,H_2}^{ACH} \varepsilon_g^{ADL} M^{ACH} c^{ACH}}\right\} \exp\left(\frac{\dot{n}_{H_2,eff,z}}{\rho D_{H_2,eff}^{ADL}/\delta^{ADL}}\right) \tag{34}$$

On substitution for $\omega_{H_2,\delta^{ACH-DL}}^{+}$ from Eq. (34) into Eq. (32), the following equation was obtained to predict ω_{H_2} as a function of the distance z in the anode reaction layer:

$$\omega_{H_2} = \alpha \left[\cosh\left(\sqrt{F_1^{A}} z\right) - \zeta \sinh\left(\sqrt{F_1^{A}} z\right)\right] \tag{35a}$$

which is valid for $\delta^{ACH-DL} < z \le \delta^{ACH-DL-RL}$ and where

$$\zeta = \tanh\left(\sqrt{F_1^{A}} \delta^{ACH-DL-RL}\right) \tag{35b}$$

and

$$\alpha = \frac{1 - \{1 - \omega_{H_2}^{ACH} + \dot{n}_{H_2,eff,z}/k_{c,H_2}\varepsilon_g^{ADL}M^{ACH}c^{ACH}\}\exp(\dot{n}_{H_2,eff,z}/\rho D_{H_2,eff}^{ADL}/\delta^{ADL})}{\cosh\left(\sqrt{F_1^A}\delta^{ACH-DL}\right)\left[1 - \tanh\left(\sqrt{F_1^A}\delta^{ACH-DL}\right)\right]\left[\tanh\left(\sqrt{F_1^A}\delta^{ACH-DL-RL}\right)\right]} \tag{35c}$$

where $\dot{n}_{H_2,eff,z} = i_{geom}M_{H_2}/2F$.

The prediction of ω_{H_2} as a function of z at an x-plane requires the data on $\dot{n}_{H_2,eff,z}$ corresponding to a geometric current density, transport and electrode electrochemical kinetic parameters, and dimensions of the anode flow channel and diffusion and reaction layers parallel to the z direction. Also, the effective diffusivity of hydrogen in the anode reaction layer, $D_{H_2,eff}^{ARL}$, appearing in Eq. (31b) is given below:

$$D_{H_2,eff}^{ARL} = \frac{D_{H_2}^{ARL}\varepsilon_g^{ARL}}{\tau_{p(g)}^{ARL}} \tag{36}$$

Eq. (35a) was used to obtain $(-d\omega_{H_2}/dz|_{z=\delta^{ACH-DL}})$ and the result substituted into Eq. (27) to obtain:

$$\dot{n}_{H_2,eff,z}^{ARL}\Big|_{z=\delta^{ACH-DL}} = \rho D_{H_2,eff}^{ARL}\alpha\sqrt{F_1^A}\left[\zeta\cosh\left(\sqrt{F_1^A}\delta^{ACH-DL}\right) - \sinh\left(\sqrt{F_1^A}\delta^{ACH-DL}\right)\right] \tag{37}$$

If at an x-plane, the required geometric current density is i_{geom}, the hydrogen mass flux that must enter the anode reaction layer at $z = \delta^{ACH-DL} = \delta^{ACH} + \delta^{ADL}$ is

$$\dot{n}_{H_2,eff,z}^{ARL}\Big|_{z=\delta^{ACH-DL}} = \left(\frac{i_{geom}}{2F}\right)M_{H_2} \tag{38}$$

On equating the right-hand sides of Eqs. (37) and (38), one obtains the following equation:

$$f_1 = \alpha\sqrt{F_1^A}\left[\zeta\cosh\left(\sqrt{F_1^A}\delta^{ACH-DL}\right) - \sinh\left(\sqrt{F_1^A}\delta^{ACH-DL}\right)\right] = \left(\frac{i_{geom}}{2F}\right)\left(\frac{M_{H_2}}{\rho D_{H_2,eff}^{ARL}}\right) \tag{39}$$

One should solve Eq. (39) for $\sqrt{F_1^A}$ for a given value of i_{geom} using a method: trial and error, Newton's or graphical method; or any commercial computer software. One can then determine the anode reaction overvoltage $|\eta^A|$ from Eq. (31b) corresponding to the geometric current density, i_{geom}.

Chemical species mole balances in the anode channel flow are now considered. Under the set of operational conditions of a reformer, when negligible amounts of carbon monoxide and oxygen are present in the fuel gas supplied to a PEMFC, the fuel feed gas mixture to the cell anode-side flow channel is assumed to contain hydrogen, nitrogen, carbon dioxide and water vapor. It is further assumed that leakage of gases through the polymer electrolyte separator from the cell anode to cathode is negligibly small. The molar flow rates (mol s^{-1}) of the chemical species, nitrogen, carbon dioxide, hydrogen, and water vapor at any x-location are given as follows:

$$\dot{N}_{\alpha}^{ACH} = \dot{N}_{\alpha,0}^{ACH} \quad (\alpha = N_2, CO_2) \tag{40}$$

$$\dot{N}_{H_2}^{ACH} = \dot{N}_{H_2,0}^{ACH} - W^{ACH}\int_0^x \frac{\dot{n}_{H_2,eff,z}}{M_{H_2}}dx \tag{41a}$$

$$= \dot{N}_{H_2,0}^{ACH} - \frac{W^{ACH}}{2F}\int_0^x i_{geom}dx \tag{41b}$$

$$= \dot{N}_{H_2,0}^{ACH} - \frac{W^{ACH}xi_{geom,ave}}{2F} \tag{41c}$$

for the assumption of

$$i_{geom} = i_{geom,ave} = \frac{\text{total cell current}}{\text{total geometric area of the cell anode}}$$

$$\dot{N}_{H_2O}^{ACH} = \dot{N}_{H_2O,0}^{ACH} \tag{42a}$$

if the cell operational conditions are such that the net loss of water from the gas mixture flow in the cell anode channel is negligible.

If the net amount of water transported from the anode to cathode side of the cell is ζ_{H_2O}, moles of water per mole of H^+ ions that move from the anode to cathode reaction layer of the cell; then, the molar flow rate of water in the cell anode channel at an x-location is given as

$$\dot{N}^{ACH}_{H_2O} = \dot{N}^{ACH}_{H_2O,0} - \frac{\zeta_{H_2O} W^{ACH}}{F} \int_0^x i_{geom} dx \tag{42b}$$

$$= \dot{N}^{ACH}_{H_2O,0} - \frac{\zeta_{H_2O} W^{ACH} x}{F} i_{geom,ave} \tag{42c}$$

for the assumption of $i_{geom} = i_{geom,ave}$.

The species molar flow rate information provided in Eqs. (40)–(42) should be used in Eqs. (13c)–(13e). If the fuel gas mixture feed to the cell anode channel contains small amounts of carbon monoxide and oxygen in addition to nitrogen, carbon dioxide, hydrogen and water vapor; then, one may use the following equations for carbon monoxide and oxygen at an x-location in the anode flow channel:

$$\dot{N}^{ACH}_{CO_2} = \dot{N}^{ACH}_{CO_2,0} + \dot{N}^{ACH}_{CO,0} \tag{43}$$

$$\dot{N}^{ACH}_{O_2} = \dot{N}^{ACH}_{O_2,0} - \tfrac{1}{2}\dot{N}^{ACH}_{CO,0} \tag{44}$$

Eqs. (43) and (44) were obtained with the assumption that the small amount of carbon monoxide present in the feed would be converted to carbon dioxide completely via the CO oxidation reaction: $CO + (1/2)O_2 \rightleftarrows CO_2$, that takes place preferentially over the hydrogen oxidation reaction at the platinum surface for temperatures less than 200 °C [35]. It is here suggested that the amount of oxygen present in the fuel feed gas mixture should be such that it is sufficient to completely convert CO at the platinum electrode surface to CO_2, particularly for high temperature phosphoric acid PEMFCs, leaving residual oxygen in the anode channel flow, $\dot{N}^{ACH}_{O_2}$, to a negligible level to prevent possible oxidation of hydrogen.

2.2. The fuel cell cathode-side formulation

The flux of O_2 in the z-direction through the gas phase concentration boundary layer prevailing at the porous surface of the carbon cathode diffusion layer (CDL) facing the cathode channel flow is given by

$$(-\dot{N}_{O_2,eff,z}) = k^{CCH}_{C,O_2} \varepsilon^{CDL}_g (c^{CCH}_{O_2} - c_{O_2,z^{CDL}_{fs}}) \tag{45}$$

The mass flux of oxygen in the z-direction through the gas phase concentration boundary layer is given by

$$(-\dot{n}_{O_2,eff,z}) = (-\dot{N}_{O_2,eff,z}) M_{O_2} = k^{CCH}_{C,O_2} \varepsilon^{CDL}_g M^{CCH} c^{CCH} (\omega^{CCH}_{O_2} - \omega_{O_2,z^{CDL}_{fs}}) \tag{46a}$$

where

$$M^{CCH} = \sum_\alpha y^{CCH}_\alpha M_\alpha \tag{46b}$$

$$y^{CCH}_\alpha = \frac{\dot{N}^{CCH}_\alpha}{\sum_\alpha \dot{N}^{CCH}_\alpha} \quad (\alpha = O_2, H_2O_{(v)}, N_2) \tag{46c}$$

$$\omega^{CCH}_\alpha = \frac{y^{CCH}_\alpha M_\alpha}{M^{CCH}} \tag{46d}$$

$$c^{CCH} = \frac{P^{CCH}}{RT} \tag{46e}$$

As with the anode channel, the cathode channel mass transfer coefficient k^{CCH}_{C,O_2} value can be determined using semiempirical equations [36,38]. The gas mixture density in the cathode channel is to be calculated from:

$$\rho = \frac{P^{CCH}}{RT} \sum_\alpha y^{ACH}_\alpha M_\alpha \quad (\alpha = O_2, N_2, H_2O \text{ mainly}) \tag{47}$$

The molar flux of $H_2O_{(v)}$ in the z-direction through the gas phase concentration boundary layer prevailing at the porous surface of the CDL is given by

$$\dot{N}_{H_2O,eff,z} = k^{CCH}_{C,H_2O} \varepsilon^{CDL}_g (c_{H_2O,z^{CDL}_{fs}} - c^{CCH}_{H_2O}) \tag{48}$$

The mass flux of $H_2O_{(v)}$ in the z-direction through the gas phase concentration boundary layer is given by

$$\dot{n}_{H_2O,\mathrm{eff},z} = \dot{N}_{H_2O,\mathrm{eff},z} M_{H_2O} = k^{CCH}_{C,HO} \varepsilon^{CDL}_{g} M^{CCH} c^{CCH} (\omega_{H_2O,z^{CDL}_{fs}} - \omega^{CCH}_{H_2O}) \tag{49}$$

From Eqs. (46a) and (49), one obtains:

$$\omega_{O_2,z^{CDL}_{fs}} = \omega^{CCH}_{O_2} - \frac{(-\dot{n}_{O_2,\mathrm{eff},z})}{k^{CCH}_{C,O_2} \varepsilon^{CDL}_{g} M^{CCH} c^{CCH}} \tag{50}$$

$$\omega_{H_2O,z^{CDL}_{fs}} = \omega^{CCH}_{H_2O} + \frac{\dot{n}_{H_2O,\mathrm{eff},z}}{k^{CCH}_{C,H_2O} \varepsilon^{CDL}_{g} M^{CCH} c^{CCH}} \tag{51}$$

The nitrogen molar flux along the z-direction is assumed zero. That is

$$\dot{N}_{N_2,\mathrm{eff},z} = 0.0 \tag{52a}$$

Also

$$\dot{n}_{N_2,\mathrm{eff},z} = \dot{N}_{N_2,\mathrm{eff},z} M_{N_2} = 0 \tag{52b}$$

The general mass flux equation, which describes the mass transport of a chemical species α in the CDL by the mass diffusion and convection processes, is given as

$$\dot{n}_{\alpha,\mathrm{eff},z} = \rho D^{CDL}_{\alpha,\mathrm{eff}} \left(\frac{-\mathrm{d}\omega_\alpha}{\mathrm{d}z} \right) + \omega_\alpha \sum_\beta \dot{n}_{\beta,\mathrm{eff},z} \quad (\alpha, \beta = O_2, H_2O, N_2) \tag{53}$$

Under the steady-state condition at an x-location:

$$\dot{n}_{O_2,\mathrm{eff},z} \ \ (\text{at any} \ \ z \ \ \text{within the CDL}) = \dot{n}_{O_2,\mathrm{eff},z}|_{z=z^{CRL}_{fs}} = -\frac{i_{\mathrm{geom}}}{4F} M_{O_2} \tag{54}$$

The water mass flux in the z-direction within the CDL at any x is given as

$$\dot{n}_{H_2O,\mathrm{eff,z}} = \frac{i_{\mathrm{geom}} M_{H_2O}}{2F} + \frac{\zeta_{H_2O} i_{\mathrm{geom}} M_{H_2O}}{F} = (1 + 2\zeta_{H_2O}) \frac{i_{\mathrm{geom}} M_{H_2O}}{2F} \tag{55}$$

Using the expressions in Eqs. (54) and (55), with $\dot{n}_{N_2,\mathrm{eff},z} = 0$:

$$\sum_\beta \dot{n}_{\beta,\mathrm{eff},z} = \dot{n}_{O_2,\mathrm{eff},z} + \dot{n}_{H_2O,\mathrm{eff},z} + \dot{n}_{N_2,\mathrm{eff},z} \tag{56a}$$

$$= \left(\frac{i_{\mathrm{geom}} M_{H_2}}{2F} \right) \left(1 + \frac{2M_{H_2O}}{M_{H_2}} \zeta_{H_2O} \right) \tag{56b}$$

$$= \left(\frac{i_{\mathrm{geom}} M_{H_2}}{2F} \right) (1 + 18\zeta_{H_2O}) \tag{56c}$$

Combining the information in Eqs. (53) and (56c) to obtain:

$$\dot{n}_{\alpha,\mathrm{eff},z} = \rho D^{CDL}_{\alpha,\mathrm{eff}} \left(\frac{-\mathrm{d}\omega_\alpha}{\mathrm{d}z} \right) + \omega_\alpha \left(\frac{i_{\mathrm{geom}} M_{H_2}}{2F} \right) (1 + 18\zeta_{H_2O}) \quad (\alpha = O_2, H_2O_{(v)}, N_2) \tag{57a}$$

where

$$D^{CDL}_{\alpha,\mathrm{eff}} = \frac{D^{CDL}_{\alpha,\mathrm{gas}} \varepsilon^{CDL}_{g}}{\tau^{CDL}_{p(g)}} \tag{57b}$$

Eq. (57a) is transformed to

$$\frac{\mathrm{d}\omega_\alpha}{\mathrm{d}z} + \left[\frac{-(1 + 18\zeta_{H_2O})(i_{\mathrm{geom}} M_{H_2}/2F)}{\rho D^{CDL}_{\alpha,\mathrm{eff}}} \right] \omega_\alpha = \frac{-\dot{n}_{\alpha,\mathrm{eff},z}}{\rho D^{CDL}_{\alpha,\mathrm{eff}}} \tag{58}$$

The analytical solution to the differential Eq. (58), with the boundary condition at $z = z_{fs}^{CDL}$ (far-side of CDL with respect to $z = 0$), $\omega_\alpha = \omega_{\alpha,fs}^{CDL}$, is given below:

$$\omega_\alpha = \omega_{\alpha,fs}^{CDL} \exp\left[\frac{(1+18\zeta_{H_2O})(i_{geom}M_{H_2}/2F)}{\rho D_{\alpha,eff}^{CDL}}(z - z_{fs}^{CDL})\right] + \frac{\dot{n}_{\alpha,eff,z}}{(1+18\zeta_{H_2O})(i_{geom}M_{H_2}/2F)} \times \left[1 - \exp\left\{\frac{(1+18\zeta_{H_2O})(i_{geom}M_{H_2}/2F)}{\rho D_{\alpha,eff}^{CDL}}(z - z_{fs}^{CDL})\right\}\right] \quad (59)$$

valid for a chemical species α in the z-range, $z_{ns}^{CDL} \le z \le z_{fs}^{CDL}$; $\alpha = O_2$, $H_2O_{(v)}$, N_2.

Eq. (59) is applied to the chemical species, N_2, O_2, and $H_2O_{(v)}$, respectively, in conjunction with Eqs. (52b), (54) and (55), to obtain:

$$\omega_{N_2} = \omega_{N_2,fs}^{CDL} \exp\left[\frac{(1+18\zeta_{H_2O})(i_{geom}M_{H_2}/2F)}{\rho D_{N_2,eff}^{CDL}}(z - z_{fs}^{CDL})\right] \quad (60)$$

$$\omega_{O_2} = \omega_{O_2,fs}^{CDL} \exp\left[\frac{(1+18\zeta_{H_2O})(i_{geom}M_{H_2}/2F)}{\rho D_{O_2,eff}^{CDL}}(z - z_{fs}^{CDL})\right] - \left(\frac{8}{1+18\zeta_{H_2O}}\right) \times \left[1 - \exp\left\{\frac{(1+18\zeta_{H_2O})(i_{geom}M_{H_2}/2F)}{\rho D_{O_2,eff}^{CDL}}(z - z_{fs}^{CDL})\right\}\right] \quad (61)$$

$$\omega_{H_2O} = \omega_{H_2O,fs}^{CDL} \exp\left[\frac{(1+18\zeta_{H_2O})(i_{geom}M_{H_2}/2F)}{\rho D_{H_2O,eff}^{CDL}}(z - z_{fs}^{CDL})\right] + 9\left(\frac{1+2\zeta_{H_2O}}{1+18\zeta_{H_2O}}\right) \times \left[1 - \exp\left\{\frac{(1+18\zeta_{H_2O})(i_{geom}M_{H_2}/2F)}{\rho D_{H_2O,eff}^{CDL}}(z - z_{fs}^{CDL})\right\}\right] \quad (62)$$

The mathematical expressions for $(-\dot{n}_{O_2,eff,z})$ and $\dot{n}_{H_2O,eff,z}$ from Eqs. (54) and (55), respectively, are substituted into Eqs. (50) and (51) to obtain the expressions for $\omega_{O_2,z_{fs}^{CDL}}$ and $\omega_{H_2O,z_{fs}^{CDL}}$. The resulting expressions for $\omega_{O_2,z_{fs}^{CDL}}$, $\omega_{H_2O,z_{fs}^{CDL}}$, and $\omega_{N_2,z_{fs}^{CDL}} = \omega_{N_2}^{CCH}$ are substituted, respectively, into Eqs. (61), (62) and (60) to obtain the following expressions:

$$\omega_{O_2} = \left[\omega_{O_2}^{CCH} - \frac{(i_{geom}M_{O_2}/4F)}{k_{C,O_2}^{CCH}\varepsilon_g^{CDL}M^{CCH}c^{CCH}}\right] \exp\left[\frac{(1+18\zeta_{H_2O})(i_{geom}M_{H_2}/2F)}{\rho D_{O_2,eff}^{CDL}}(z - z_{fs}^{CDL})\right] - \frac{8}{1+18\zeta_{H_2O}}\left[1 - \exp\left\{\frac{(1+18\zeta_{H_2O})(i_{geom}M_{H_2}/2F)}{\rho D_{O_2,eff}^{CDL}}(z - z_{fs}^{CDL})\right\}\right] \quad (63)$$

$$\omega_{H_2O} = \left[\omega_{H_2O}^{CCH} + \frac{(1+2\zeta_{H_2O})(i_{geom}M_{H_2O}/2F)}{k_{C,H_2O}^{CCH}\varepsilon_g^{CDL}M^{CCH}c^{CCH}}\right] \exp\left[\frac{(1+18\zeta_{H_2O})(i_{geom}M_{H_2}/2F)}{\rho D_{H_2O,eff}^{CDL}}(z - z_{fs}^{CDL})\right] + 9\left(\frac{1+2\zeta_{H_2O}}{1+18\zeta_{H_2O}}\right) \times \left[1 - \exp\left\{\frac{(1+18\zeta_{H_2O})(i_{geom}M_{H_2}/2F)}{\rho D_{H_2O,eff}^{CDL}}(z - z_{fs}^{CDL})\right\}\right] \quad (64)$$

$$\omega_{N_2} = \omega_{N_2,fs}^{CDL} \exp\left[\frac{(1+18\zeta_{H_2O})(i_{geom}M_{H_2}/2F)}{\rho D_{N_2,eff}^{CDL}}(z - z_{fs}^{CDL})\right] \quad (65a)$$

where

$$\omega_{N_2,fs}^{CDL} = \omega_{N_2}^{CCH} - \frac{i_{geom}}{4F\varepsilon_g^{CDL}M^{CCH}c^{CCH}}\left[(2+4\zeta_{H_2O})\frac{M_{H_2O}}{k_{c,H_2O}^{CCH}} - \frac{M_{O_2}}{k_{c,O_2}^{CCH}}\right] \quad (65b)$$

The Eqs. (63)–(65a) can be used to predict the mass fraction profiles of oxygen, water vapor and nitrogen in the gas-filled pores of the cathode diffusion layer (CDL) for $z_{ns}^{CDL} \le z \le z_{fs}^{CDL}$. The mass fractions of the chemical species oxygen, water, and nitrogen at

the interface between the CRL and CDL, but on the CDL-side, are obtained by setting $z = z_{ns}^{CDL}$, with $(z_{ns}^{CDL} - z_{fs}^{CDL}) = -\delta^{CDL}$.

$$\omega^{+}_{O_2,z_{ns}^{CDL}} = \left[\omega_{O_2}^{CCH} - \frac{(i_{geom}M_{O_2}/4F)}{k_{C,O_2}^{CCH}\varepsilon_g^{CDL}M^{CCH}c^{CCH}}\right]\exp\left[\frac{-(1+18\zeta_{H_2O})(i_{geom}M_{H_2}/2F)}{\rho D_{O_2,eff}^{CDL}}\delta^{CDL}\right] - \frac{8}{1+18\zeta_{H_2O}} \times \left[1-\exp\left\{\frac{-(1+18\zeta_{H_2O})(i_{geom}M_{H_2}/2F)}{\rho D_{O_2,eff}^{CDL}}\delta^{CDL}\right\}\right] \quad (66)$$

$$\omega^{+}_{H_2O,z_{ns}^{CDL}} = \left[\omega_{H_2O}^{CCH} + \frac{(1+2\zeta_{H_2O})(i_{geom}M_{H_2O}/2F)}{k_{C,H_2O}^{CCH}\varepsilon_g^{CDL}M^{CCH}c^{CCH}}\right]\exp\left[\frac{-(1+18\zeta_{H_2O})(i_{geom}M_{H_2}/2F)}{\rho D_{H_2O,eff}^{CDL}}\delta^{CDL}\right] + 9\left(\frac{1+2\zeta_{H_2O}}{1+18\zeta_{H_2O}}\right) \times \left[1-\exp\left\{\frac{-(1+18\zeta_{H_2O})(i_{geom}M_{H_2}/2F)}{\rho D_{H_2O,eff}^{CDL}}\delta^{CDL}\right\}\right] \quad (67)$$

$$\omega^{+}_{N_2,z_{ns}^{CDL}} = \omega_{N_2,fs}^{CDL}\exp\left[\frac{-(1+18\zeta_{H_2O})(i_{geom}M_{H_2}/2F)\delta^{CDL}}{\rho D_{N_2,eff}^{CDL}}\right] \quad (68)$$

In the cathode reaction layer, oxygen is transported as well as reduced via the electrochemical reaction given by Eq. (2) at the catalyst platinum-electrolyte active sites-(s) to produce water. If the first electron transfer step, $O_2 - s + H^+ + e^- \rightarrow HO_2 - s$, is assumed to be the rate-limiting step in the kinetic mechanism of the overall oxygen reduction process, the oxygen reduction rate per unit active surface area of the electrocatalyst is given by

$$(-r_{O_2}) = \left(\frac{i_{0,s}^{C}}{4F}\right)\exp\left(\frac{\alpha_c^{C}|\eta^{C}|F}{RT}\right) \quad (69)$$

where the cathodic exchange current density, $i_{0,s}^{C}$, is given by

$$i_{0,s}^{C} = i_{0,s,T_0,p_{O_2},0}^{C}\exp\left[\frac{E_0^{C}}{R}\left(\frac{1}{T_0}-\frac{1}{T}\right)\right]\left(\frac{p_{O_2}}{p_{O_2,0}}\right)^{n} \quad (70)$$

For the first electron transfer step as the kinetic rate-limiting elementary step, the reaction order, $n = 1$ [41]:

$$|\eta^{C}| = |E^{C} - E_{rev}^{C}| = \left|(\Delta\phi)^{C} - (\Delta\phi_{rev})^{C}\right| = |(\phi_{Pt} - \phi_{electrolyte})^{C} - (\phi_{Pt} - \phi_{electrolyte})_{rev}^{C}| \quad (71)$$

where E^{C} is the actual voltage at the cathode reaction layer (V).

For the assumption of spherical crystallites of the platinum catalyst, with average size, r_{Pt}^{C} (radius); the platinum surface area per unit mass of the catalyst is given by

$$s^{C} = \frac{3}{r_{Pt}^{C}\rho_{Pt}} \quad (72)$$

If some fraction of the platinum catalyst surface is not in contact with the electroactive regions of the polymer electrolyte; then, the reaction effective electrocatalyst interfacial area is given by

$$s_{eff}^{C} = a_{eff}^{C}s^{C} \quad (73)$$

If the catalyst Pt loading in the cathode reaction layer is m_{Pt}^{C}, the electrochemical reaction active electrocatalyst surface area per unit cathode reaction layer volume is

$$a^{C} = s_{eff}^{C}m_{Pt}^{C} \quad (74)$$

The relation of m_{Pt}^{C} to the catalyst loading per unit geometric area, $m_{Pt,geom}^{C}$, of the cathode reaction layer is given as

$$m_{Pt,geom}^{C} = \delta^{C}m_{Pt}^{C}, [(\text{g Pt})\text{cm}_{geom}^{-2}] \quad (75)$$

The molar oxygen consumption rate, via the cathodic electrochemical reaction, per unit cathode reaction layer (CRL) volume is given by

$$-R^{\mathrm{C}}_{\mathrm{O}_2} = \left(\frac{i^{\mathrm{C}}_{0,\mathrm{s}}}{4F}\right) a^{\mathrm{C}} \exp\left(\frac{\alpha^{\mathrm{C}}_{\mathrm{c}}|\eta^{\mathrm{C}}|F}{RT}\right) \tag{76}$$

The oxygen consumption rate, in mass units, in the CRL is given by

$$-R^{\mathrm{C}}_{\mathrm{O}_2,\mathrm{mass}} = \left(\frac{i^{\mathrm{C}}_{0,\mathrm{s}}}{4F}\right) a^{\mathrm{C}} M_{\mathrm{O}_2} \exp\left(\frac{\alpha^{\mathrm{C}}_{\mathrm{c}}|\eta^{\mathrm{C}}|F}{RT}\right) \tag{77}$$

Oxygen diffuses toward the solid polymer electrolyte separator layer along z-coordinate in the direction of decreasing z while being reduced by the electrochemical reaction at the electrocatalyst interface effective active sites. Based on the coupled oxygen transport and electrochemical reduction processes, a differential model equation describing the oxygen mass fraction variation with distance z, obtained by the application of steady-state oxygen mass balance over a spatial element, is given by

$$\rho D^{\mathrm{CRL}}_{\mathrm{O}_2,\mathrm{eff}} \frac{\mathrm{d}^2\omega_{\mathrm{O}_2}}{\mathrm{d}z^2} = (-R^{\mathrm{C}}_{\mathrm{O}_2,\mathrm{mass}}) \tag{78}$$

In the derivation of Eq. (78), the product of gas mixture density and effective oxygen mass diffusivity, i.e. $\rho D^{\mathrm{CDL}}_{\mathrm{O}_2,\mathrm{eff}}$, was assumed invariant with respect to z in the thin cathode reaction layer (CRL). The gas mixture density, ρ, may be taken equal to that in the cathode channel gas mixture at an x-location as a first approximation. The gas mixture density at an x-location can be computed from Eq. (47). The effective oxygen mass diffusivity, $D^{\mathrm{CRL}}_{\mathrm{O}_2,\mathrm{eff}}$, in the cathode reaction layer is given by

$$D^{\mathrm{CRL}}_{\mathrm{O}_2,\mathrm{eff}} = \frac{D^{\mathrm{CRL}}_{\mathrm{O}_{2(\mathrm{g})}} \varepsilon^{\mathrm{CRL}}_{\mathrm{g}}}{\tau^{\mathrm{CRL}}_{\mathrm{p(g)}}} \tag{79}$$

and

$$\varepsilon^{\mathrm{CRL}}_{\mathrm{g}} = 1 - (\varepsilon^{\mathrm{CRL}}_{\mathrm{Pt}} + \varepsilon^{\mathrm{CRL}}_{\mathrm{C}} + \varepsilon^{\mathrm{CRL}}_{\mathrm{SPE}} + \varepsilon^{\mathrm{CRL}}_{\mathrm{other}}) \tag{80}$$

If the gas-filled average pore radius in the CRL is less than 100 Å, $D^{\mathrm{CRL}}_{\mathrm{O}_{2(\mathrm{g})}}$ should be corrected for the Knudsen effect.

Assuming a first-order reaction with respect to oxygen ($n = 1$) and using the expression for $i_{0,\mathrm{s}}$ in Eq. (70); the oxygen consumption rate per unit CRL volume, Eq. (77) leads to

$$(-R^{\mathrm{C}}_{\mathrm{O}_2,\mathrm{mass}}) = \left(\frac{i_{0,\mathrm{s},T_0,p_{\mathrm{O}_2},0} M^{\mathrm{CCH}} a^{\mathrm{C}}}{4F}\right) \left(\frac{P^{\mathrm{CCH}}}{p_{\mathrm{O}_2,0}}\right) \exp\left\{\frac{E^{\mathrm{C}}_0}{R}\left(\frac{1}{T_0} - \frac{1}{T}\right) + \frac{\alpha^{\mathrm{C}}_{\mathrm{c}}|\eta^{\mathrm{C}}|F}{RT}\right\} \omega_{\mathrm{O}_2} \tag{81}$$

Substitution for $(-R^{\mathrm{C}}_{\mathrm{O}_2,\mathrm{mass}})$ from (81) into (78) leads to

$$\frac{\mathrm{d}^2\omega_{\mathrm{O}_2}}{\mathrm{d}z^2} = F^{\mathrm{C}}_1 \omega_{\mathrm{O}_2} \tag{82a}$$

where

$$F^{\mathrm{C}}_1 = \left(\frac{i^{\mathrm{C}}_{0,\mathrm{s},T_0,p_{\mathrm{O}_2}} a^{\mathrm{C}} M^{\mathrm{CCH}}}{4F(\rho^{\mathrm{CCH}} D^{\mathrm{CRL}}_{\mathrm{O}_2,\mathrm{eff}})}\right) \left(\frac{P^{\mathrm{CCH}}}{p_{\mathrm{O}_2,0}}\right) \exp\left\{\frac{E^{\mathrm{C}}_0}{R}\left(\frac{1}{T_0} - \frac{1}{T}\right) + \frac{\alpha^{\mathrm{C}}_{\mathrm{c}}|\eta^{\mathrm{C}}|F}{RT}\right\} \tag{82b}$$

For the isothermal condition, with the assumption of constant $|\eta^{\mathrm{C}}|$ in the relatively thin cathode reaction layer, Eq. (82a) was solved using the following boundary conditions:

$$z = z^{\mathrm{CRL}}_{\mathrm{ns}}, \qquad \left(\frac{\mathrm{d}\omega_{\mathrm{O}_2}}{\mathrm{d}z}\right)^{+} = 0 \tag{83a}$$

and

$$z = z^{\mathrm{CRL}}_{\mathrm{fs}}, \qquad \omega_{\mathrm{O}_2} = \omega^{\mathrm{CRL}-}_{\mathrm{O}_2,\mathrm{fs}} \tag{83b}$$

where $\omega^{\mathrm{CRL}-}_{\mathrm{O}_2,\mathrm{fs}}$ = mass fraction of oxygen on the negative side of the interface between the CRL and CDL. The solution to the differential Eq. (82a) is given as

$$\omega_{\mathrm{O}_2} = \alpha_1 \left[\cosh\left(\sqrt{F^{\mathrm{C}}_1} z\right) - \zeta_1 \sinh\left(\sqrt{F^{\mathrm{C}}_1} z\right)\right] \tag{84a}$$

where

$$\alpha_1 = \frac{\omega_{O_2,fs}^{CRL-}}{\cosh\left(\sqrt{F_1^C} z_{fs}^{CRL}\right)\left[1 - \tanh\left(\sqrt{F_1^C} z_{ns}^{CRL}\right)\tanh\left(\sqrt{F_1^C} z_{fs}^{CRL}\right)\right]} \tag{84b}$$

valid for $z_{ns}^{CRL} \le z \le z_{fs}^{CRL}$.

In general (activity of oxygen on the negative-side of the interface between the CRL and CDL) = (activity of oxygen on the positive-side of the interface between the CRL and CDL), with the assumption of equilibrium with respect to oxygen at the interface. However, for the presence of gas phase in the pores of CRL and CDL, it is quite reasonable to assume:

$$\omega_{O_2,fs}^{CRL-} = \omega_{O_2,z_{ns}^{CDL}}^{+} \tag{85}$$

Using the information provided for $\omega_{O_2,z_{ns}^{CDL}}^{+}$ in Eq. (66) in conjunction with Eq. (85), Eq. (84b) becomes:

$$\alpha_1 = \frac{[\omega_{O_2}^{CCH} - (i_{geom} M_{O_2}/4F)/k_{C,O_2}^{CCH}\varepsilon_g^{CDL} M^{CCH} c^{CCH}]\exp[-(1+18\zeta_{H_2O})(i_{geom} M_{H_2}/2F)\delta^{CDL}/\rho D_{O_2,eff}^{CDL}]}{\cosh\left(\sqrt{F_1^C} z_{fs}^{CRL}\right)\left[1 - \tanh\left(\sqrt{F_1^C} z_{ns}^{CRL}\right)\tanh\left(\sqrt{F_1^C} z_{fs}^{CRL}\right)\right]}$$
$$- \frac{(8/(1+18\zeta_{H_2O}))[1 - \exp\{-(1+18\zeta_{H_2O})(i_{geom} M_{H_2}/2F)\delta^{CDL}/(\rho D_{O_2,eff}^{CDL})\}]}{\cosh\left(\sqrt{F_1^C} z_{fs}^{CRL}\right)\left[1 - \tanh\left(\sqrt{F_1^C} z_{ns}^{CRL}\right)\tanh\left(\sqrt{F_1^C} z_{fs}^{CRL}\right)\right]} \tag{86}$$

$$\zeta_1 = \tanh\left(\sqrt{F_1^C} z_{ns}^{CRL}\right) \tag{87}$$

Eq. (84a) can be employed to predict the oxygen mass fraction profile in the cathode reaction layer as a function of distance z. At an x-plane, the oxygen mass flux along the z-direction is given by

$$(-\dot{n}_{O_2,eff,z}) = \rho^{CCH} D_{O_2,eff}^{CRL}\left(\left.\frac{d\omega_{O_2}}{dz}\right|_{z=z_{fs}^{CRL}}\right) \tag{88a}$$

$$= \frac{i_{geom} M_{O_2}}{4F} \tag{88b}$$

Using the information provided for ω_{O_2} in Eqs. (84a), in conjunction with Eqs. (88a) and (88b), the following result is obtained:

$$\frac{i_{geom} M_{O_2}}{4F} = \rho^{CCH} D_{O_2,eff}^{CRL}\left(\alpha_1\sqrt{F_1^C}\right)\left[\sinh\left(\sqrt{F_1^C} z_{fs}^{CRL}\right) - \zeta_1\cosh\left(\sqrt{F_1^C} z_{fs}^{CRL}\right)\right] \tag{89}$$

Eq. (89) can be re-arranged as

$$\left(\frac{i_{geom} M_{O_2}}{4F\rho^{CCH} D_{O_2,eff}^{CRL}}\right) = \left(\alpha_1\sqrt{F_1^C}\right)\left[\sinh\left(\sqrt{F_1^C} z_{fs}^{CRL}\right) - \zeta_1\cosh\left(\sqrt{F_1^C} z_{fs}^{CRL}\right)\right] \tag{90}$$

For the steady operation of a fuel cell, Eq. (90) can be solved for F_1^C by a trial-error or graphical procedure for a fixed value of i_{geom} at an x-plane. Then, using the defining Eq. (82b) for F_1^C, one can obtain the cathodic electrochemical reaction activation voltage loss, $|\eta^C|$, for a fixed i_{geom} value at an x-plane. Also, one can find the average cathodic activation voltage loss, $|\eta^C|_{ave}$ using the cell average geometric current density. This rigorous mathematical formulation shows how one can obtain the activation voltage loss at the cathode reaction layer by taking into account the effect of mass transport of oxygen through the various layers of the cell on the CRL side.

The chemical species mole flow rates at the cathode channel inlet, $x = 0$ plane, are given by $\dot{N}_{i,0}^{CCH}$, ($i = O_2, H_2O, N_2$). Under the cell steady-state, isothermal operational conditions, the chemical species molar flow rates in the cathode channel at an x-plane are given as follows:

$$\dot{N}_{O_2,x}^{CCH} = \dot{N}_{O_2,0}^{CCH} - \frac{W^{CCH}}{4F}\int_0^x i_{geom}\,dx \tag{91a}$$

with $i_{\text{geom}} = i_{\text{geom,ave}}$:

$$\dot{N}^{\text{CCH}}_{\text{O}_2,x} = \dot{N}^{\text{CCH}}_{\text{O}_2,0} - \frac{W^{\text{CCH}} x i_{\text{geom,ave}}}{4F} \tag{91b}$$

$$\dot{N}^{\text{CCH}}_{\text{H}_2\text{O},x} = \dot{N}^{\text{CCH}}_{\text{H}_2\text{O},0} + \left(\frac{1+2\zeta_{\text{H}_2\text{O}}}{2F}\right) W^{\text{CCH}} \int_0^x i_{\text{geom}}\,\text{d}x \tag{92a}$$

$$= \dot{N}^{\text{CCH}}_{\text{H}_2\text{O},0} + (1+2\zeta_{\text{H}_2\text{O}}) \left(\frac{W^{\text{CCH}} x i_{\text{geom,ave}}}{2F}\right) \tag{92b}$$

$$\dot{N}^{\text{CCH}}_{\text{N}_2} = \dot{N}^{\text{CCH}}_{\text{N}_2,0} \tag{93}$$

The total gas mixture molar flow rate in the cathode flow channel at an x-plane is given by

$$\dot{N}^{\text{CCH}}_{\text{t}} = \sum_i \dot{N}^{\text{CCH}}_{i,x} = \sum_i \dot{N}^{\text{CCH}}_{i,0} + (1+4\zeta_{\text{H}_2\text{O}}) \frac{W^{\text{CCH}} \int_0^x i_{\text{geom}}\,\text{d}x}{4F} \tag{94a}$$

and, with $i_{\text{geom}} = i_{\text{geom,ave}}$:

$$= \sum_i \dot{N}^{\text{CCH}}_{i,0} + (1+4\zeta_{\text{H}_2\text{O}}) \frac{W^{\text{CCH}} x i_{\text{geom,ave}}}{4F} \tag{94b}$$

Mole and weight (or mass) fractions of chemical species at an x-plane in the cathode flow channel are, respectively, given by

$$y^{\text{CCH}}_i = \frac{\dot{N}^{\text{CCH}}_{i,x}}{\dot{N}^{\text{CCH}}_t} \tag{95a}$$

$$= \frac{\dot{N}^{\text{CCH}}_{i,x}}{\sum_i \dot{N}^{\text{CCH}}_{i,0} + (W^{\text{CCH}}/4F)(1+4\zeta_{\text{H}_2\text{O}}) \int_0^x i_{\text{geom}}\,\text{d}x} \tag{95b}$$

with $i_{\text{geom}} = i_{\text{geom,ave}}$ and $i = \text{O}_2$, $\text{H}_2\text{O}_{(\text{v})}$, N_2:

$$y^{\text{CCH}}_i = \frac{\dot{N}^{\text{CCH}}_{i,x}}{\sum_i \dot{N}^{\text{CCH}}_{i,0} + (1+4\zeta_{\text{H}_2\text{O}})(W^{\text{CCH}} x i_{\text{geom,ave}}/4F)} \tag{95c}$$

$$\omega^{\text{CCH}}_i = \frac{\dot{N}^{\text{CCH}}_{i,x} M_i}{\sum_i \dot{N}^{\text{CCH}}_{i,x} M_i} \tag{96a}$$

$$= \frac{\dot{N}^{\text{CCH}}_{i,x} M_i}{\sum_i \dot{N}^{\text{CCH}}_{i,0} M_i + W^{\text{CCH}}(1+\zeta_{\text{H}_2\text{O}} M_{\text{H}_2\text{O}}) \int_0^x i_{\text{geom}}\,\text{d}x/F} \tag{96b}$$

with $i_{\text{geom}} = i_{\text{geom,ave}}$ and $i = \text{O}_2$, $\text{H}_2\text{O}_{(\text{v})}$, N_2:

$$\omega^{\text{CCH}}_i = \frac{\dot{N}^{\text{CCH}}_{i,x} M_i}{\sum_i \dot{N}^{\text{CCH}}_{i,0} M_i + (1+\zeta_{\text{H}_2\text{O}} M_{\text{H}_2\text{O}})(W^{\text{CCH}} x i_{\text{geom,ave}}/F)} \tag{96c}$$

The oxygen weight fraction at an x-plane in the cathode flow channel, as provided by Eq. (96b) or (96c), is to be used in Eq. (86) to calculate the parameter α_1 for its subsequent use in Eq. (90) to calculate the parameter F^{C}_1; hence, the activation voltage loss, $|\eta^{\text{C}}|$ at an x-plane. Eq. (96c) can be used to compute the oxygen mass (or weight) fraction, $\omega^{\text{CCH}}_{\text{O}_2,x}$, as a function of distance x in the cathode channel. Then, the average weight fraction of oxygen, $\omega^{\text{CCH}}_{\text{O}_2,\text{ave}}$, can be calculated from the following equation:

$$\omega^{\text{CCH}}_{\text{O}_2,\text{ave}} = \frac{\int_{x=0}^{x=L^{\text{CCH}}} \omega^{\text{CCH}}_{\text{O}_2}\,\text{d}x}{L^{\text{CCH}}} \tag{97}$$

The average oxygen weight fraction, $\omega^{\text{CCH}}_{\text{O}_2,\text{ave}}$, should then be used to calculate the average activation voltage loss at the cathode reaction layer, $|\eta^{\text{C}}|_{\text{ave}}$, for an average geometric current density of $i_{\text{geom,ave}}$ using Eqs. ((90), with $i_{\text{geom}} = i_{\text{geom,ave}}$), ((86), with $\omega^{\text{CCH}}_{\text{O}_2} = \omega^{\text{CCH}}_{\text{O}_2,\text{ave}}$, $i_{\text{geom}} = i_{\text{geom,ave}}$), and ((82b), with $|\eta^{\text{C}}| = |\eta^{\text{C}}|_{\text{ave}}$).

3. Application of the developed formulation

The formulation provided in Section 2 may be employed to calculate an average cell voltage at a given or desired average current density for a hydrogen/air PEMFC, using an acid electrolyte medium, for example, Nafion–Teflon–$Zr(HPO_4)_2$ composite[41], PBO/PBI doped with phosphoric acid, or sulfonated poly(arylene ether sulfone) [42]. Example cell operational conditions can be an elevated temperature of 110 °C, 1 atm total pressure, with the water vapor partial pressure less than saturated vapor pressure in the anode-side hydrogen fuel stream and 50% or even lower relative humidity in the cathode-side oxidant air stream to maintain oxygen partial pressure at a sufficiently high level to prevent excessive activation voltage loss at the cathode reaction layer. One should determine the total ohmic voltage loss, $\eta^{t}_{\Omega,ave}$, for a desired average current density, $i_{geom,ave}$, using Eqs. (7)–(12a). The average activation voltage losses, $|\eta^{A}|_{ave}$ and $|\eta^{C}|_{ave}$ can be calculated using Eqs. (39) and (90). The average reversible cell voltage, $E^{cell}_{rev,ave}$, should be calculated using Eq. (4) at the arithmetic average of the partial pressure values of hydrogen, oxygen, and water vapor at the anode and cathode channel inlets and exits. Then, the cell actual average voltage can be computed from the following equation:

$$V^{cell}_{ave} = E^{cell}_{rev,ave} - \eta^{t}_{\Omega,ave} - (|\eta^{A}|_{ave} + |\eta^{C}|_{ave}) - \eta^{m} \tag{98}$$

It is here noted that the mass transport related voltage loss, η^m, should be set equal to zero if the $E^{cell}_{rev,ave}$ is computed at the arithmetic average of the partial pressure values of hydrogen, oxygen, and water vapor at the anode and cathode channel inlets and exits as they prevail at the anode and cathode reaction layers. If $E^{cell}_{rev,ave}$ is computed at the average of these species partial pressures as they prevail in the channel flow streams; then there may still be some need to apply a mass transport correction through the use of an empirical equation such as [39]:

$$\eta^m = m \exp(n i_{geom}) \tag{99}$$

where $m = 2.11 \times 10^{-5}$ V, $n = 8\,cm^2_{geom}\,A^{-1}$, i_{geom} in $(A\,cm^2_{geom})$.

The effect of hydrogen fuel crossover from the cell anode to cathode on the cell open circuit voltage is significant [39]. For example, if the hydrogen crossover flux corresponds to the internal current density (≡(no. of g mol of hydrogen diffusing from the anode to cathode reaction layer, through the electrolyte separator layer, per unit geometric area per s) × ($2F$ coulomb per mole of hydrogen crossover)) = 1 $(mA\,cm^2_{geom})$, the open circuit cell voltage is about 0.97 V instead of the thermodynamic reversible voltage of 1.2 V at 25 °C. In the practical current density range of $i_{geom} \geq 100\,mA\,cm^2_{geom}$, the effect of hydrogen crossover on the cell operating efficiency is not of great significance depending upon the diffusion characteristics of the membrane separator layer. One can compute the voltage loss due to the hydrogen crossover flux using the simple approach given in Ref. [39].

4. Single cell electric power and thermal efficiency

Corresponding to a desired average geometric current density, $i_{geom,ave}$, the total cell current (A), is given by

$$I^{cell}_{t} = i_{geom,ave}\,(L^{ACH} W^{ACH}) \tag{100}$$

where L^{ACH} and W^{ACH} are the dimensions of the anode electrode parallel to the x- and y-coordinates as shown in Fig. 1. The magnitude of the cell electric power (W), is given by

$$|\dot{W}^{cell}_{electric}| = V^{cell}_{ave} I^{cell}_{t} \tag{101}$$

Hydrogen consumption rate in the cell $(mol\,s^{-1})$:

$$(-\Delta \dot{N}^{cell}_{H_2}) = \frac{I^{cell}_{t}}{2F} \tag{102}$$

Rate of thermal energy production if the entire amount of hydrogen consumed in the cell were combusted:

$$\Delta \dot{H}^{cell}_{t} = (-\Delta \dot{N}^{cell}_{H_2}) \Delta H_T = \left(\frac{I^{cell}_{t}}{2F}\right) \Delta H_T \tag{103}$$

where ΔH_T is the enthalpy of the hydrogen oxidation reaction, Eq. (3), at the cell temperature, T (K). For the gas mixture ideal gas behavior, $\Delta H_T = \Delta H^{\circ}_T = \sum_i \nu_i H^{\circ}_{i,T}$ = standard-state enthalpy of the reaction, Eq. (3), at the cell temperature, T, per g mol of hydrogen oxidized to water vapor $(J\,mol^{-1})$. Eq. (103) now becomes:

$$\Delta \dot{H}^{cell}_{t} = \left(\frac{I^{cell}_{t}}{2F}\right) \Delta H^{\circ}_T \tag{104}$$

ΔH_T° (J mol^{-1}) is given by [36]:

$$\Delta H_T^\circ = \sum_i \nu_i \Delta H_{f,i,T_0}^\circ + R\left[\Delta A(T-T_0) + \frac{\Delta B}{2}(T^2 - T_0^2) + \frac{\Delta C}{3}(T^3 - T_0^3) - \Delta D\left(\frac{1}{T} - \frac{1}{T_0}\right)\right] \tag{105}$$

where $R = 8.314$ (J mol^{-1} K^{-1}); $T_0 = 298.15$ K; $\nu_{H_2(g)} = -1$, $\nu_{O_2(g)} = -1/2$, $\nu_{H_2O(g)} = 1$; $\Delta H_{f,H_2,T_0}^\circ = \Delta H_{f,O_2,T_0}^\circ = 0$ (J mol^{-1}), $\Delta H_{f,H_2O,T_0}^\circ = -241818$ (J mol^{-1}); $\Delta A = \sum_i \nu_i A_i = -1.5985$, $\Delta B = \sum_i \nu_i B_i = 0.775 \times 10^{-3}$ K^{-1}, $\Delta C = \sum_i \nu_i C_i = 0.0$ K^{-2}, $\Delta D = \sum_i \nu_i D_i = 0.130421 \times 10^5$ K^2, where A_i, B_i, C_i, D_i are the heat capacity coefficients of an ideal gas i.

The single cell thermal efficiency is defined as

$$\eta_{thermal}^{cell} = \frac{-\left|\dot{W}_{electric}^{cell}\right|}{\Delta \dot{H}_t^{cell}} = \frac{2FV_{ave}^{cell}}{(-\Delta H_T^\circ)} \tag{106}$$

Thermal energy that must be removed from the cell:

$$|\dot{Q}_{remove}^{cell}| = (1 - \eta_{thermal}^{cell})(-\Delta \dot{H}_t^{cell}) \tag{107}$$

to maintain the cell at a desired temperature, T.

5. Extension of the single cell formulation for the performance prediction of a stack of identical cells connected in series (steady-state, isothermal operation)

It is here assumed that the anode-side flow channels of the individual PEMFCs connected in series are fed with the identical rates of fuel (hydrogen or a gas mixture, containing hydrogen, from a fuel reformer). The cathode-side flow channels of the individual PEMFCs are also fed with the identical rates of oxidant, air. The fuel and oxidant (air) flows are in the same (i.e. parallel) flow direction. For the cells connected in series, the same amount of total current passes through each cell. That is to say that

$$I_t^{cell} = I_t^{stack} \tag{108}$$

where I_t^{stack} = total current from a stack of PEMFCs connected in series. For n PEMFCs connected in series in a stack, the total stack voltage is given by

$$V_t^{stack} = nV_{ave}^{cell} \tag{109}$$

where a single cell average voltage is obtained from Eq. (98). The cell stack electric power output is given by

$$|\dot{W}_{electric}^{stack}| = V_t^{stack} I_t^{stack} = nV_{ave}^{cell} I_t^{stack} \tag{110}$$

The hydrogen fuel consumption rate per cell which is equal to the rate of decrease in hydrogen molar flow rate in the cell anode-side flow channel is given by

$$-\Delta \dot{N}_{H_2} = \frac{I_t^{cell}}{2F} = \frac{I_t^{stack}}{2F} \tag{111}$$

The total hydrogen fuel consumption rate in the cell stack of n cells connected in series is given by

$$-\Delta \dot{N}_{H_2}^t = n(-\Delta \dot{N}_{H_2}) = \frac{nI_t^{stack}}{2F} \tag{112}$$

The thermal energy production rate is given by the following equation if the entire amount of hydrogen fuel consumed in the cell stack were combusted (i.e. oxidized to water vapor):

$$\Delta \dot{H}_t^{stack} = (-\Delta \dot{N}_{H_2}^t)\Delta H_T^\circ \tag{113a}$$

$$= \left(\frac{nI_t^{stack}}{2F}\right)\Delta H_T^\circ \tag{113b}$$

The cell stack thermal efficiency is given by

$$\eta_{thermal}^{stack} = \frac{-\left|\dot{W}_{electric}^{stack}\right|}{\Delta \dot{H}_t^{stack}} = \frac{2FV_{ave}^{cell}}{(-\Delta H_T^\circ)} = \eta_{thermal}^{cell} \tag{114}$$

Notice that the cell stack thermal efficiency is equal to a single cell thermal efficiency for a set of identical single cells connected in series operating under the isothermal, steady-state conditions. Total heat removal rate from the cell stack to maintain its temperature at a desired level of T is given by

$$|\dot{Q}^{\text{stack}}_{\text{remove}}| = (1 - \eta^{\text{stack}}_{\text{thermal}})(-\Delta \dot{H}^{\text{stack}}_{\text{t}}) \tag{115a}$$

$$= (1 - \eta^{\text{stack}}_{\text{thermal}}) \left(\frac{n I^{\text{stack}}_{\text{t}}}{2F} \right) (-\Delta H^{\circ}_{T}) \tag{115b}$$

where n is the number of identical PEMFCs connected in series.

The total molar flow rate of a chemical species i at the cell stack inlet to provide fuel to the anode-side channel of each cell in the stack is represented by $\dot{N}^{\text{ACH,stack}}_{\text{in},i}$ ($i = \text{H}_2$, $\text{H}_2\text{O}_{(\text{v})}$ for humid hydrogen feed or $i = \text{H}_2$, $\text{H}_2\text{O}_{(\text{v})}$, CO_2, N_2, etc. for fuel feed to the cell stack from a fuel reformer). Total molar flow rate of a chemical species i at the cell stack inlet to provide oxidant (air) to the cathode-side channel of each cell in the stack is represented by $N^{\text{CCH,stack}}_{\text{in},i}$ ($i = \text{O}_2$, $\text{H}_2\text{O}_{(\text{v})}$, N_2 for humid air feed). Total chemical species molar flow rates at the cell stack fuel- and oxidant-side exits are given as follows:

$$\dot{N}^{\text{ACH,stack}}_{\text{exit,H}_2} = \dot{N}^{\text{ACH,stack}}_{\text{in,H}_2} - \frac{n I^{\text{stack}}_{\text{t}}}{2F} \tag{116a}$$

$$\dot{N}^{\text{ACH,stack}}_{\text{exit,H}_2\text{O}_{(\text{v})}} = \dot{N}^{\text{ACH,stack}}_{\text{in,H}_2\text{O}} - n \left(\frac{I^{\text{stack}}_{\text{t}} \zeta_{\text{H}_2\text{O}}}{F} \right) \tag{116b}$$

$$\dot{N}^{\text{ACH,stack}}_{\text{exit},i} = \dot{N}^{\text{ACH,stack}}_{\text{in},i} \quad (i = \text{CO}_2, \text{N}_2, \text{etc.}) \tag{116c}$$

$$\dot{N}^{\text{CCH,stack}}_{\text{exit,O}_2} = \dot{N}^{\text{CCH,stack}}_{\text{in,O}_2} - \frac{n I^{\text{stack}}_{\text{t}}}{4F} \tag{116d}$$

$$\dot{N}^{\text{CCH,stack}}_{\text{exit,H}_2\text{O}_{(\text{v})}} = \dot{N}^{\text{CCH,stack}}_{\text{in,H}_2\text{O}_{(\text{v})}} + n \left[(1 + 2\zeta_{\text{H}_2\text{O}}) \frac{I^{\text{stack}}_{\text{t}}}{2F} \right] \tag{116e}$$

$$\dot{N}^{\text{CCH,stack}}_{\text{exit,N}_2} = \dot{N}^{\text{CCH,stack}}_{\text{in,N}_2} \tag{116f}$$

The total gas mixture molar flow rates at the stack channel exits are given as follows:

$$\dot{N}^{\text{ACH,stack}}_{\text{exit,t}} = \sum_i \dot{N}^{\text{ACH,stack}}_{\text{exit},i} = \sum_i \dot{N}^{\text{ACH,stack}}_{\text{in},i} - n \left[(1 + 2\zeta_{\text{H}_2\text{O}}) \frac{I^{\text{stack}}_{\text{t}}}{2F} \right] \quad (i = \text{H}_2, \text{H}_2\text{O}_{(\text{v})}, \text{CO}_2, \text{N}_2, \text{etc.}) \tag{117a}$$

$$\dot{N}^{\text{CCH,stack}}_{\text{exit,t}} = \sum_i \dot{N}^{\text{CCH,stack}}_{\text{exit},i} = \sum_i \dot{N}^{\text{CCH,stack}}_{\text{in},i} + n \left[(1 + 4\zeta_{\text{H}_2\text{O}}) \frac{I^{\text{stack}}_{\text{t}}}{4F} \right] \quad (i = \text{O}_2, \text{H}_2\text{O}_{(\text{v})}, \text{N}_2) \tag{117b}$$

6. Concluding remarks

Development of a mathematical model to simulate the performance of a PEMFC at an elevated temperature has been presented. The presented model is deemed sufficiently rigorous, yet not unwieldy for its application. Effect of the reactant species mass transport on the electrochemical kinetic reaction rates in the cell anode and cathode reaction layers have been properly accounted for to correctly predict the electrochemical reaction overvoltages or activation voltage losses in the cell thin reaction layers. The single cell developed model formulation has been linked to the stack model equations to predict the performance of a stack of a number of identical PEMFCs connected in series. Provided the sufficiently accurate values of the mass transport, charge transport, and electrochemical kinetic parameters are made available, the presented model formulation can be employed to numerically simulate the performance of a single PEMFC as well as of a stack of a number of identical PEMFCs connected in series, utilizing an electrolyte such as sulfonated polyarylene ether, PBO/PBI doped with phosphoric acid, or Nafion–Teflon–$\text{Zr(HPO}_4)_2$, at an elevated temperature ($\geq$100 °C) for the isothermal and steady-state operating conditions.

References

[1] J.J. Baschuk, X. Li, J. Power Sources 86 (2000) 181–196.
[2] D.M. Bernardi, J. Electrochem. Soc. 137 (1990) 3344–3350.
[3] D.M. Bernardi, M.W. Verbrugge, J. Electrochem. Soc. 139 (1992) 2477–2491.
[4] M. Eikerling, Y.I. Kharkats, A.A. Kornyshev, Y.M. Volkovich, J. Electrochem. Soc. 145 (1998) 2684–2699.

[5] G. Maggio, V. Recupero, L. Pino, J. Power Sources 101 (2001) 275–286.
[6] A. Rowe, X. Li, J. Power Sources 102 (2001) 82–96.
[7] T.E. Springer, T.A. Zawodzinski, S. Gottesfeld, J. Electrochem. Soc. 138 (1991) 2334–2342.
[8] M. Wohr, K. Bolwin, W. Schnurnberger, M. Fischer, W. Neubrand, G. Eigenberger, Int. J. Hydrogen Energy 23 (1998) 213–218.
[9] H.P.L.H.V. Bussel, F.G.H. Koene, R.K.A.M. Mallant, J. Power Sources 71 (1998) 218–222.
[10] P. Costamagna, Chem. Eng. Sci. 56 (2001) 323–332.
[11] K. Dannenberg, P. Ekdunge, G. Lindbergh, J. Appl. Electrochem. 30 (2000) 1377–1387.
[12] V. Gurau, H. Liu, S. Kakac, AIChE J. 44 (1998) 2410–2422.
[13] I.M. Hsing, P. Futerko, Chem. Eng. Sci. 55 (2000) 4209–4218.
[14] T.V. Nguyen, R.E. White, J. Electrochem. Soc. 140 (1993) 2178–2186.
[15] K. Scott, S. Kraemer, K. Sundmacher, Inst. Chem. Eng. Symp. Ser. (1999) 11–20.
[16] N.P. Siegel, M.W. Ellis, D.J. Nelson, M.R.V. Spakovsky, J. Power Sources 128 (2004) 173–184.
[17] D. Singh, D.M. Lu, N. Djilaki, Int. J. Eng. Sci. 37 (1999) 431–452.
[18] G. Squadrito, G. Maggio, E. Passalacqua, F. Lufrano, A. Patti, J. Appl. Electrochem. 29 (1999) 1449–1455.
[19] S. Um, C.Y. Wang, K.S. Chen, J. Electrochem. Soc. 147 (2000) 4485–4493.
[20] J.S. Yi, T.V. Nguyen, J. Electrochem. Soc. 145 (1998) 1149–1159.
[21] J.S. Yi, T.V. Nguyen, J. Electrochem. Soc. 146 (1999) 38–45.
[22] T. Berning, N. Djilali, Three dimensional computational analysis of transport phenomena in a PEM fuel cell, in: Proceedings of the Seventh Grove Fuel Cell Symposium, London, 2001.
[23] T. Berning, N. Djilali, J. Power Sources 106 (2002) 284–294.
[24] T. Berning, N. Djilali, J. Power Sources 124 (2003) 440–452.
[25] S. Dutta, S. Shimpalee, J.W.V. Zee, J. Appl. Electrochem. 29 (1999) 135–146.
[26] S. Dutta, S. Shimpalee, J.W.V. Zee, Int. J. Heat Mass Transfer 44 (2001) 2001.
[27] T.C. Jen, T. Yan, S.H. Chan, Int. J. Heat Mass Transfer 46 (2003) 4157–4168.
[28] H.N. Neshat, S. Shimpalee, S. Dutta, W.K. Lee, J.W.V. Zee, Proc. ASME Adv. Energy Syst. Div. 39 (1999) 337–350.
[29] P.T. Nguyen, T. Berning, N. Djilali, J. Power Sources 130 (2004) 149–157.
[30] S.M. Senn, D. Poulikakos, Three dimensional computational modeling of polymer electrolyte fuel cells, in: Proceedings of the Fuel Cell Research Symposium—Modeling and Experimental Validation, 2004.
[31] S. Shimpalee, S. Dutta, W.K. Lee, J.W.V. Zee, Proc. ASME Heat Transfer Div. 364 (1) (1999) 367–374.
[32] S. Um, C.Y. Wang, J. Power Sources 125 (2004) 40–51.
[33] T. Zhou, H. Liu, Int. J. Transport Phenomena 3 (2001) 177–198.
[34] K.W. Lum, J.J. McGuirk, J. Power Sources 143 (2005) 103–124.
[35] S.S. Sandhu, Y.A. Saif, J.P. Fellner, J. Power Sources 140 (2005) 88–102.
[36] S.S. Sandhu, Fuel cell development for AEF and PAD applications, University of Dayton, 2004, pp. 7-1–7-68.
[37] J.M. Smith, H.C.V. Ness, M.M. Abbot, Introduction to Chemical Engineering Thermodynamics, McGraw-Hill, NY, 2005, pp. 494–495.
[38] W.L. McCabe, J.C. Smith, P. Harriott, Unit Operations of Chemical Engineering, McGraw-Hill, New York, 1993, p. 1130.
[39] J. Larminie, Fuel Cell Systems Explained, Wiley, Chichester, West Sussex, 2003, p. 406.
[40] R.B. Bird, W.E. Stewart, E.N. Lightfoot, Transport Phenomena, John Wiley and Sons, NY, 2002, p. 583.
[41] Y. Si, H.R. Kunz, J.M. Fenton, J. Electrochem. Soc. 151 (2004) A623–A631.
[42] C. Ma, L. Zhang, S. Mukerjee, D. Ofer, B. Nair, J. Membr. Sci. 219 (2003).